Editors' Suggestion | Featured in Physics

Measurement of Motion beyond the Quantum Limit by Transient Amplification

R. D. Delaney,[1,2,*] A. P. Reed,[1,2,3] R. W. Andrews,[1,2,4] and K. W. Lehnert[1,2,5]
[1]JILA, Boulder, Colorado 80309, USA
[2]Department of Physics, University of Colorado, Boulder, Colorado 80309, USA
[3]Honeywell Quantum Solutions, Broomfield, Colorado 80021, USA
[4]HRL Laboratories, LLC, Malibu, California 90265, USA
[5]National Institute of Standards and Technology, Boulder, Colorado 80309, USA

(Received 2 August 2019; published 30 October 2019)

Through simultaneous but unequal electromechanical amplification and cooling processes, we create a method for a nearly noiseless pulsed measurement of mechanical motion. We use transient electromechanical amplification (TEA) to monitor a single motional quadrature with a total added noise -8.5 ± 2.0 dB relative to the zero-point motion of the oscillator, or equivalently the quantum limit for simultaneous measurement of both mechanical quadratures. We demonstrate that TEA can be used to resolve fine structure in the phase space of a mechanical oscillator by tomographically reconstructing the density matrix of a squeezed state of motion. Without any inference or subtraction of noise, we directly observe a squeezed variance 2.8 ± 0.3 dB below the oscillator's zero-point motion.

DOI: 10.1103/PhysRevLett.123.183603

The past ten years have seen a dramatic improvement in the ability to measure and control the quantum state of macroscopic mechanical oscillators. Much of this progress results from advances in the parametric coupling of these oscillators to optical cavities or resonant electrical circuits. These related fields of optomechanics and electromechanics have demonstrated the ability to cool mechanical oscillators to near their motional ground state [1], entangle mechanical oscillators with each other [2,3] or with other degrees of freedom [4], and create squeezed states of motion [5–7]. To verify the successful creation of these nonclassical states, electromechanical and optomechanical methods have also enabled measurements of mechanical motion with near 50% quantum efficiency [8,9], or equivalently an added noise equal to the zero-point motion of the oscillator, the quantum limit for simultaneous measurement of both mechanical quadratures [10].

These advances have encouraged notions of using nonclassical states of motion to test quantum mechanics at larger scales, sensing forces with quantum enhanced precision, and enabling quantum transduction between disparate physical systems [11]. But as mechanical oscillators are prepared in more profoundly quantum states [12,13], with finer features in oscillator phase space, the measurement efficiency must further improve to resolve these fine features and to use them to realize a quantum advantage.

Reaching higher levels of efficiency with existing methods is hindered by fundamental and technical limitations, which seem difficult to overcome. In electromechanical and optomechanical devices, the state of motion can be converted without gain or added noise into a propagating electric field, and one quadrature component of the field can be measured nearly noiselessly [4,8]. However, the loss experienced by the field traveling between the device and the amplifier has prevented quantum efficiency much greater than 50%. To improve measurement efficiency, the device can be used as its own parametric amplifier, emitting an electric field that encodes an amplified copy of the mechanical oscillator's state, thereby overcoming any subsequent loss and inefficiency of the following measurement chain. Using this strategy, both quadratures can be measured simultaneously with added noise very close to the quantum limit [9]. For steady state monitoring of a single quadrature, backaction evading schemes are, in principle, noiseless [6,14]. However, unwanted parametric effects, both parasitic [15,16] and intrinsic to the electromechanical Hamiltonian [17–19], have prevented measurements with noise far below the quantum-limited value.

In this Letter, we implement an efficient measurement of a single mechanical quadrature, monitoring mechanical motion with an added noise of -8.5 ± 2.0 dB relative to zero-point motion, and a quantum efficiency of $\eta_q = 88 \pm 5\%$. By generating mechanical dynamics equivalent to the time reverse of dissipative squeezing [20], we intentionally induce mechanical instability through the electromechanical interaction, allowing for a pulsed measurement of the initial state of the mechanical oscillator. We term this protocol transient electromechanical amplification (TEA), and demonstrate the resolution of fine features in phase space by using TEA to perform quantum state tomography [21] on a dissipatively squeezed state of the mechanical oscillator, from which we reconstruct the mechanical density matrix.

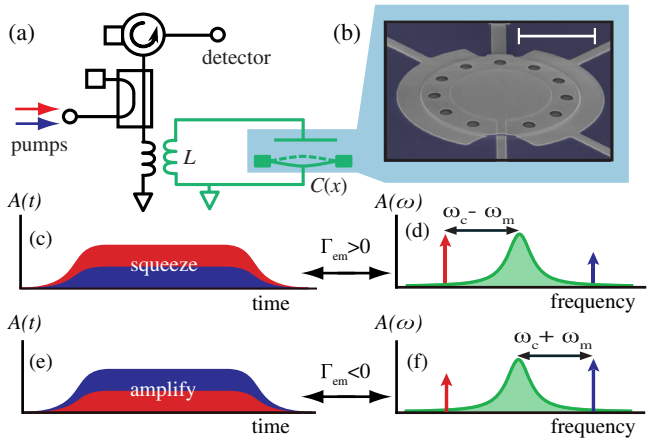

FIG. 1. (a) Schematic of experiment consisting of the electromechanical circuit (green) inductively coupled to a transmission line. Pump tones are applied through a directional coupler, while outgoing microwave signals are directed to a chain of conventional microwave amplifiers and mixer circuits, forming a microwave receiver, which adds noise much larger than zero-point fluctuations. (b) False-color micrograph of aluminum drum. The white bar corresponds to a distance of approximately 10 μm. (c) Time and (d) frequency domain representation of temporally overlapping dissipative squeezing pump tone amplitudes [$A(t)$ and $A(\omega)$]. (e) Time and (f) frequency domain representation of transient electromechanical amplification (TEA) pump tone amplitudes.

The device [shown schematically in Fig. 1(a)] is an aluminum inductor-capacitor (LC) circuit composed of a spiral inductor and a compliant vacuum gap capacitor, which couples electrical energy to motion. The LC circuit has a resonant frequency of $\omega_c \approx 2\pi \times 7.4$ GHz, and is coupled to a transmission line at a rate $\kappa_{\text{ext}} \approx 2\pi \times 3.1$ MHz. The compliant top-plate of the capacitor [shown in Fig. 1(b)] is free to vibrate with a fundamental mechanical resonant frequency of $\omega_m \approx 2\pi \times 9.4$ MHz and mechanical linewidth of $\Gamma_m \approx 2\pi \times 21$ Hz. For additional device parameters and details, see the Supplemental Material [17]. The electromechanical system is attached to the base plate of a dilution refrigerator, resulting in a mechanical occupancy of $n_m \leq 40$ in thermal equilibrium.

The electromechanical circuit is in the resolved sideband regime [22], enabling coherent control of motion with microwave tones. Applying a red detuned microwave pump to the LC circuit ($\Delta \equiv \omega_c - \omega_p = -\omega_m$) allows for sideband cooling [1], and state transfer between mechanical and microwave fields [23,24], where ω_p is the frequency of the pump tone. A blue detuned microwave pump ($\Delta = +\omega_m$) creates entanglement between mechanical and microwave fields [4], and realizes a quantum limited phase-insensitive amplifier of mechanical motion [9]. Combining these two interactions, with simultaneous application of red and blue detuned pump tones, addresses two orthogonal mechanical quadratures $X_+ = i(b^\dagger - b)/\sqrt{2}$ and $X_- = (b^\dagger + b)/\sqrt{2}$ independently, and enables backaction evading measurement, dissipative squeezing, and TEA.

The type of interaction is determined by the sign of $\Gamma_{\text{em}}(t) = \Gamma_-(t) - \Gamma_+(t)$, where $\Gamma_\pm(t)$ are the electromechanical growth and decay rates caused by the blue (+) and red (-) detuned microwave tones, respectively [4]. Dissipative squeezing occurs when $\Gamma_{\text{em}}(t) > 0$, which cools the mechanical oscillator towards a squeezed vacuum state [20]. The microwave control tones that enable dissipative squeezing are shown schematically in the time and frequency domain in Figs. 1(c) and 1(d). Ideal backaction evasion occurs when $\Gamma_{\text{em}} = 0$, where perfect constructive interference between sidebands decouples one mechanical quadrature from microwave vacuum fluctuations, producing a noiseless representation of a single mechanical quadrature in a single microwave quadrature [25]. Finally, TEA occurs when $\Gamma_{\text{em}}(t) < 0$, amplifying motion with energy gain $G \approx e^{|\Gamma_{\text{em}}|t}$. Figures 1(e) and 1(f) show the microwave pump tones used in the time and frequency domain for TEA.

For both TEA and backaction evading measurement, the motion of a single mechanical quadrature X is encoded in a single microwave quadrature U. The variance of U can then be written as the sum of the noise contributions from the signal and added noise:

$$\langle \Delta U^2 \rangle = G_{\text{tot}}(\langle \Delta X^2 \rangle + \langle \Delta X^2_{\text{add}} \rangle), \tag{1}$$

where G_{tot} is the total gain of the microwave receiver chain in units of V^2/quanta. If the total added measurement noise $\langle \Delta X^2_{\text{add}} \rangle$ is known, then the variance of the mechanical state $\langle \Delta X^2 \rangle$ can be inferred. Equivalently, by preparing a mechanical state with known variance the added measurement noise can be characterized. For an ideal single quadrature measurement $\langle \Delta X^2_{\text{add}} \rangle = 0$ and U faithfully records one quadrature of the mechanical state. Approaching this ideal behavior is highly desirable for characterizing quantum states of motion, as the number of repeated measurements required to reconstruct a quantum state grows rapidly with added noise. Furthermore, assigning meaningful uncertainties to the extracted density matrix after any inference or deconvolution procedure is complicated and subtle, diminishing confidence in the inferred state.

For the two special quadratures $X_\pm$, the noise properties of TEA are determined by the relative strength of Γ_+ and Γ_-. Assuming optimal detuning of the microwave tones by exactly $\pm\omega_m$ and $\Gamma_\pm \ll \kappa/2$ (avoiding the strong coupling regime), the added noise $\langle \Delta X^2_{\text{add},\pm} \rangle$ referred to the input of TEA is given by

$$\langle \Delta X^2_{\text{add},\pm} \rangle \approx \frac{(\sqrt{\Gamma_+} \pm \sqrt{\Gamma_-})^2 + \Gamma_m(2n_m + 1)}{2|\Gamma_{\text{em}} + \Gamma_m|}. \tag{2}$$

In analogy with the high cooperativity limit, if $\Gamma_m(2n_m + 1)/|\Gamma_{\text{em}} + \Gamma_m| \ll 1$, then $\langle \Delta X^2_{\text{add},-} \rangle$ will be less

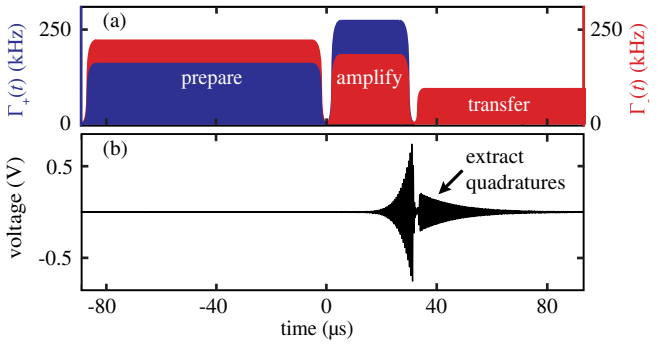

FIG. 2. (a) General pulse protocol for characterization of TEA and squeezing. The first overlapping red- or blue-detuned pulses determine whether the mechanical oscillator is squeezed, cooled, or allowed to thermalize with its environment. The second set of pulses tune the gain and added noise of the measurement. The final red-detuned pulse transfers the amplified state of the mechanical oscillator to the microwave field for quadrature extraction. The pulse lengths are chosen so that $e^{|\Gamma_{\rm em}|t}$ is large, and provides sufficient amplification gain or dissipative squeezing and cooling to overwhelm the thermal noise of the mechanical environment. The pulse envelopes drawn are slower than in the experiment for visual clarity. (b) A single experimental voltage trace of the down-converted microwave field ($\omega_{\rm het} = 2\pi \times 1.8$ MHz) showing the resulting exponential growth and decay of the microwave field due to the amplification and transfer pulses respectively.

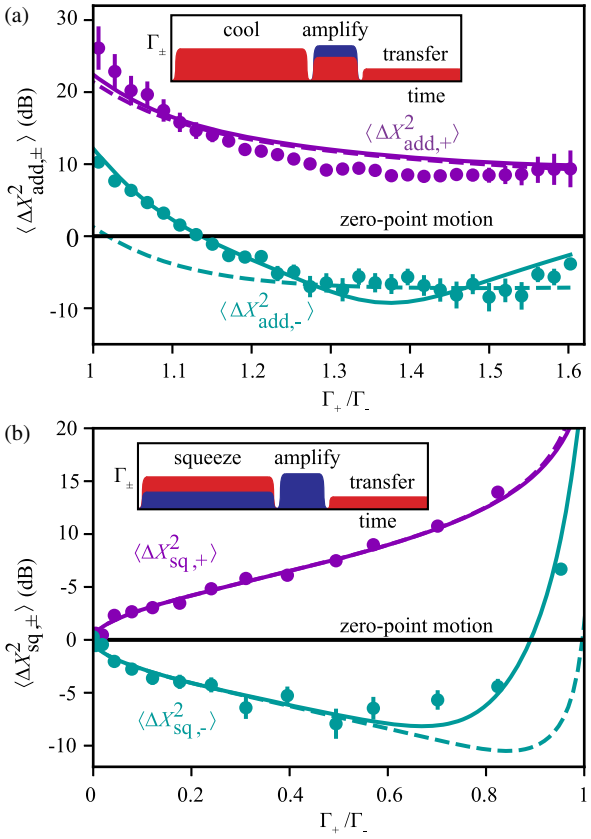

FIG. 3. (a) Total added noise referred to the input of TEA relative to zero-point motion. Γ_+ is varied, while $\Gamma_- = 2\pi \times 181$ kHz is held constant. The circles are data, while theory from Eq. (2) (including HEMT noise contributions) is shown without any free parameters as the dashed lines, and deviates significantly because the pump power is large enough to induce additional parametric processes. The solid lines are theory including parametric effects (with free parameters) [17]. The inset illustrates the pulse sequence used for the inference of $\langle \Delta X^2_{\rm add,\pm} \rangle$. Here, we obtain a minimum added noise of $\langle \Delta X^2_{\rm add,-} \rangle = -8.5 \pm 2.0$ dB. (b) Inferred variance of the squeezed $\langle \Delta X^2_{\rm sq,-} \rangle$ and anti-squeezed $\langle \Delta X^2_{\rm sq,+} \rangle$ quadratures after dissipatively squeezing. Γ_+ is varied, while $\Gamma_- = 2\pi \times 154$ kHz is held constant. The minimum squeezed variance is $\langle \Delta X^2_{\rm sq,-} \rangle = -7.9 \pm 1.4$ dB. The circles are the data, while theory is shown without any free parameters as the dashed lines, with the expected agreement at low pump powers. The solid lines are theory including parametric effects (with free parameters) [17]. The inset illustrates the pulse sequence for the inference of squeezing.

than zero-point motion. In the case where $\Gamma_- = 0$, equal noise will be added to both quadratures, enabling nearly quantum limited phase-insentive amplification [9]. However, if the pump frequencies deviate from optimal detuning, either through an initial detuning, or through pump-power induced shifts in the resonance frequency of the circuit, Eq. (2) is not valid, and theory including pump induced mechanical and cavity frequency shifts is required [17]. Similarly, the variance of the squeezed and anti-squeezed quadratures after dissipative squeezing $\langle \Delta X^2_{\rm sq,\pm} \rangle$ takes the same form as Eq. (2), but with $\Gamma_- > \Gamma_+$.

In Fig. 2(a) we demonstrate, in a three-step protocol, the control of the mechanical oscillator needed to study TEA. An initial pair of pulses prepares the mechanical oscillator in a desired state, by either sideband cooling ($\Gamma_- > 0$ and $\Gamma_+ = 0$), dissipatively squeezing ($\Gamma_- > \Gamma_+ > 0$), or letting the mechanical oscillator reach equilibrium with its thermal environment ($\Gamma_+ = \Gamma_- = 0$). Following state preparation, the motion of the mechanical oscillator and the amplitude of the microwave field are amplified by applying red and blue pumps such that $\Gamma_+ > \Gamma_-$. After a short delay, the red-detuned pump is pulsed on to transfer the previously amplified state of the mechanical oscillator to the microwave field [24]. After further amplification by a high electron-mobility transistor (HEMT) amplifier, and a room temperature measurement chain, the signal is mixed down to a heterodyne frequency of $\omega_{\rm het} = 2\pi \times 1.8$ MHz MHz, allowing the two mechanical quadratures to be extracted from the exponentially decaying microwave field shown in Fig. 2(b).

We determine experimentally the total noise $\langle \Delta X^2_{\rm add,\pm} \rangle$ added during TEA by separately preparing the mechanical oscillator in both a thermal state and through sideband cooling. By comparing the variance of these two states in a ratio, the added noise can be inferred [17,26]. Figure 3(a) shows the total added noise as a function of the ratio of red

and blue pump power. With the optimal ratio of the red and blue-detuned pumps we find total added noise relative to zero-point motion of $\langle \Delta X^2_{\mathrm{add},-} \rangle = -8.5 \pm 2.0$ dB, which is equivalent to a quantum efficiency of $\eta_q = (1 + 2\langle \Delta X^2_{\mathrm{add},-} \rangle)^{-1} = 88 \pm 5\%$. We compare these results to the prediction of Eq. (2) with no adjustable parameters, illustrating poor quantitative agreement. We attribute this discrepancy to additional squeezing of the mechanical oscillator caused by nonlinear mixing of the microwave pumps. We find good agreement in a fit to a more general theory that includes such processes [17,19]. The two theories deviate significantly from each other, but TEA nevertheless achieves a minimum added noise equivalent to that predicted by the ideal case in Eq. (2). We emphasize that $\langle \Delta X^2_{\mathrm{add},\pm} \rangle$ is the total noise added by the entire measurement chain, and for $\Gamma_+/\Gamma_- > 1.3$ TEA has large enough gain to overwhelm the noise added by the HEMT amplifier [17].

Avoiding the noise associated with the simultaneous measurement of noncommuting observables is of particular importance when measuring mechanical states with a width in phase space less than the zero-point motion of the oscillator [27], and is desirable for many quantum state tomography protocols [28]. Thus, to test the effectiveness of TEA on states with variance below zero-point fluctuations, we prepare squeezed states of motion using the dissipative procedure illustrated in the inset of Fig. 3(b). To infer the total amount of squeezing, the motion is first squeezed for 90 μs, then a 30 μs blue-detuned microwave pulse ($\Gamma_+ = 2\pi \times 73$ kHz and $\Gamma_- = 0$) is applied to amplify both motional quadratures. The variance associated with zero-point motion, which must be added by the phase-insensitive amplifier, is subtracted to infer the variance of the squeezed and antisqueezed quadratures, which is shown in Fig. 3(b). We obtain a maximum inferred vacuum squeezing of $\langle \Delta X^2_{\mathrm{sq},-} \rangle = 7.9 \pm 1.4$ dB below the zero-point motion of the mechanical oscillator. We are able to far surpass the so-called steady state 3 dB squeezing limit both because we are using pulsed operations, and more than a single mode is involved during dissipative squeezing [29]. Theory without any free parameters is plotted as the dashed lines in Fig. 3(b), which agrees well at low pump powers. The solid lines show predicted squeezing when including additional parametric effects induced by nonlinear mixing of the two microwave pumps (with free parameters) [17].

Having demonstrated that we can prepare a squeezed state with variance below zero-point motion, the ability of TEA to resolve fine phase space features can be tested by performing quantum state tomography on the squeezed mechanical state. By rotating a noiseless single quadrature measurement through all possible measurement axes, a set of phase space marginals can be recorded, and the density matrix can be reconstructed via quantum state tomography [30–34]. Figures 4(a) and 4(b) show histograms of a sideband cooled ($n_{\mathrm{sb}} \approx 0.02$) and a dissipatively squeezed

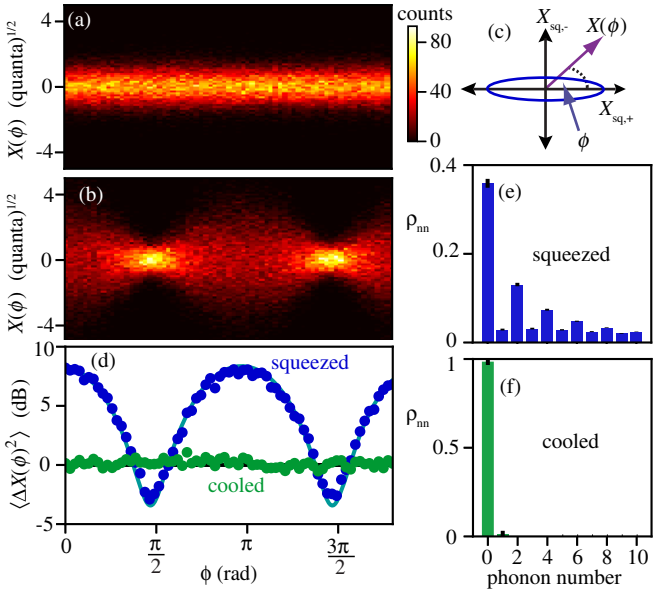

FIG. 4. Measurement of mechanical squeezed and sideband cooled states with single quadrature TEA. (a) A density plot of the marginal distributions of a sideband cooled state as a function of tomography angle ϕ. (b) A density plot of the marginal distributions of a squeezed state using single quadrature TEA as a function of ϕ. (c) The schematic shows the rotation of the single quadrature measurement axis $X(\phi)$ relative to the prepared squeezed state. The squeezed variance is represented as the blue ellipse. (d) The total measured variance of a sideband cooled state with $n_{\mathrm{sb}} \approx 0.02$ (green) and squeezed vacuum (blue), which exhibits squeezing 2.8 ± 0.3 dB below zero-point motion. The data points are the circles, while theory (with no free parameters) is the solid line. (e) Squeezed and (f) sideband cooled diagonal density matrix elements are inferred from tomographic reconstruction of the covariance matrix. The errorbars represent 90% confidence intervals estimated with an empirical bootstrap of the tomography data.

state of the mechanical oscillator as a function of the tomography angle ϕ. Figure 4(c) demonstrates the rotation of the single quadrature measurement axis relative to the prepared squeezed state by ϕ.

The minimum width that can be resolved in the tomography data $\langle \Delta X_{\mathrm{min}}(\phi)^2 \rangle$ is an important figure of merit for single quadrature measurements in the quantum regime. In Fig. 4(d) the total variance as a function of tomography angle is computed with theory (using independently measured parameters) shown as the solid blue line. The squeezed quadrature has a total variance of $\langle \Delta X_{\mathrm{min}}(\phi)^2 \rangle = \langle \Delta X^2_{\mathrm{sq},-} \rangle + \langle \Delta X^2_{\mathrm{add},-} \rangle = 2.8 \pm 0.3$ dB below the zero-point motion of the mechanical oscillator. We emphasize that this represents the total reduction in noise that is present at the end of our conventional microwave receiver and no noise is subtracted to find this result.

The marginal distributions (1.4×10^5 points in total) can be used to reconstruct the density matrix of the quantum state in the number basis. For a general quantum state, iterative

methods of tomographic reconstruction [21]—based upon maximum likelihood—are a reliable method of estimating quantum states [28], and are guaranteed to produce a physical density matrix. However, tomographic reconstruction of squeezed states in the Fock basis requires estimating density matrix elements up to very high phonon number [33,35]. To avoid calculating large density matrices we assume Gaussian Wigner quasiprobability distributions [36], and estimate the density matrix through reconstruction of the covariance matrix [37]. The covariance matrix is then used to infer the Fock basis density matrix of the mechanical oscillator. In Figs. 4(e) and 4(f) we plot the inferred diagonal density matrix elements for the squeezed vacuum and sideband cooled states, with the error bars on the measurements representing 90% confidence intervals from an empirical bootstrap procedure [17,38]. From the density matrix we also infer the purity of the squeezed state to be $\mu \equiv 1/(1+2n_{\mathrm{sq}}) = 0.53 \pm 0.03$ [17], where n_{sq} is the equivalent thermal occupation of the squeezed state. This demonstrates the direct resolution of features in phase space with a width approximately half that of zero-point fluctuations and the ability to resolve the squeezed character in the number basis.

Mechanical devices are increasingly being integrated into circuit QED systems as resource efficient elements, transducers and quantum memories, which offer access to new regimes of circuit QED [12,13]. By directly using mechanical instability as a probe, TEA can efficiently measure motion in the presence of additional nonlinear effects. Combining TEA with already demonstrated [9] quantum state transfer techniques provides a path towards efficient tomography of non-Gaussian states in macroscopic mechanical oscillators.

We acknowledge funding from AFOSR MURI Grant No. FA9550-15-1-0015, from ARO CQTS Grant No. 67C-1098620, and NSF under Grant No. PHYS 1734006. We thank Lucas Sletten for help with the experiment. We thank Brad Moores, John Teufel, and Shlomi Kotler for many useful comments on the manuscript.

*robert.delaney@colorado.edu

[1] J. D. Teufel, T. Donner, D. Li, J. W. Harlow, M. S. Allman, K. Cicak, A. J. Sirois, J. D. Whittaker, K. W. Lehnert, and R. W. Simmonds, Sideband cooling of micromechanical motion to the quantum ground state, Nature (London) **475**, 359 (2011).

[2] C. F. Ockeloen-Korppi, E. Damskägg, J.-M. Pirkkalainen, M. Asjad, A. A. Clerk, F. Massel, M. J. Woolley, and M. A. Sillanpää, Stabilized entanglement of massive mechanical oscillators, Nature (London) **556**, 478 (2018).

[3] R. Riedinger, A. Wallucks, I. Marinković, C. Löschnauer, M. Aspelmeyer, S. Hong, and S. Gröblacher, Remote quantum entanglement between two micromechanical oscillators, Nature (London) **556**, 473 (2018).

[4] T. A. Palomaki, J. D. Teufel, R. W. Simmonds, and K. W. Lehnert, Entangling mechanical motion with microwave fields, Science **342**, 710 (2013).

[5] E. E. Wollman, C. U. Lei, A. J. Weinstein, J. Suh, A. Kronwald, F. Marquardt, A. A. Clerk, and K. C. Schwab, Quantum squeezing of motion in a mechanical resonator, Science **349**, 952 (2015).

[6] F. Lecocq, J. B. Clark, R. W. Simmonds, J. Aumentado, and J. D. Teufel, Quantum Nondemolition Measurement of a Nonclassical State of a Massive Object, Phys. Rev. X **5**, 041037 (2015).

[7] J. M. Pirkkalainen, E. Damskägg, M. Brandt, F. Massel, and M. A. Sillanpää, Squeezing of Quantum Noise of Motion in a Micromechanical Resonator, Phys. Rev. Lett. **115**, 243601 (2015).

[8] M. Rossi, D. Mason, J. Chen, Y. Tsaturyan, and A. Schliesser, Measurement-based quantum control of mechanical motion, Nature (London) **563**, 53 (2018).

[9] A. P. Reed, K. H. Mayer, J. D. Teufel, L. D. Burkhart, W. Pfaff, M. Reagor, L. Sletten, X. Ma, R. J. Schoelkopf, E. Knill, and K. W. Lehnert, Faithful conversion of propagating quantum information to mechanical motion, Nat. Phys. **13**, 1163 (2017).

[10] C. M. Caves, Quantum limits on noise in linear amplifiers, Phys. Rev. D **26**, 1817 (1982).

[11] A. P. Higginbotham, P. S. Burns, M. D. Urmey, R. W. Peterson, N. S. Kampel, B. M. Brubaker, G. Smith, K. W. Lehnert, and C. A. Regal, Harnessing electro-optic correlations in an efficient mechanical converter, Nat. Phys. **14**, 1038 (2018).

[12] Y. Chu, P. Kharel, T. Yoon, L. Frunzio, P. T. Rakich, and R. J. Schoelkopf, Creation and control of multi-phonon fock states in a bulk acoustic-wave resonator, Nature (London) **563**, 666 (2018).

[13] B. A. Moores, L. R. Sletten, J. J. Viennot, and K. W. Lehnert, Cavity Quantum Acoustic Device in the Multimode Strong Coupling Regime, Phys. Rev. Lett. **120**, 227701 (2018).

[14] C. U. Lei, A. J. Weinstein, J. Suh, E. E. Wollman, A. Kronwald, F. Marquardt, A. A. Clerk, and K. C. Schwab, Quantum Nondemolition Measurement of a Quantum Squeezed State Beyond the 3 db Limit, Phys. Rev. Lett. **117**, 100801 (2016).

[15] J. Suh, M. D. Shaw, H. G. LeDuc, A. J. Weinstein, and K. C. Schwab, Thermally induced parametric instability in a back-action evading measurement of a micromechanical quadrature near the zero-point level, Nano Lett. **12**, 6260 (2012).

[16] J. Suh, A. J. Weinstein, and K. C. Schwab, Optomechanical effects of two-level systems in a back-action evading measurement of micro-mechanical motion, Appl. Phys. Lett. **103**, 052604 (2013).

[17] See Supplemental Material at http://link.aps.org/supplemental/10.1103/PhysRevLett.123.183603 for details about theory, variance calibrations and the experimental setup.

[18] J. Q. Liao, C. K. Law *et al.*, Parametric generation of quadrature squeezing of mirrors in cavity optomechanics, Phys. Rev. A **83**, 033820 (2011).

[19] I. Shomroni, A. Youssefi, N. Sauerwein, L. Qiu, P. Seidler, D. Malz, A. Nunnenkamp, and T. J. Kippenberg, Two-tone

optomechanical instability in backaction-evading measurements, arXiv:1812.11022.
[20] A. Kronwald, F. Marquardt, and A. A. Clerk, Arbitrarily large steady-state bosonic squeezing via dissipation, Phys. Rev. A **88**, 063833 (2013).
[21] A. I. Lvovsky and M. G. Raymer, Continuous-variable optical quantum-state tomography, Rev. Mod. Phys. **81**, 299 (2009).
[22] M. Aspelmeyer, T. J. Kippenberg, and F. Marquardt, Cavity optomechanics, Rev. Mod. Phys. **86**, 1391 (2014).
[23] R. W. Andrews, A. P. Reed, K. Cicak, J. D. Teufel, and K. W. Lehnert, Quantum-enabled temporal and spectral mode conversion of microwave signals, Nat. Commun. **6**, 10021 (2015).
[24] T. A. Palomaki, J. W. Harlow, J. D. Teufel, R. W. Simmonds, and K. W. Lehnert, Coherent state transfer between itinerant microwave fields and a mechanical oscillator, Nature (London) **495**, 210 (2013).
[25] A. A. Clerk, F. Marquardt, and K. Jacobs, Back-action evasion and squeezing of a mechanical resonator using a cavity detector, New J. Phys. **10**, 095010 (2008).
[26] D. M. Pozar, *Microwave Engineering* (John Wiley & Sons, New York, 2009).
[27] B. Yurke and D. Stoler, Generating Quantum Mechanical Superpositions of Macroscopically Distinguishable States via Amplitude Dispersion, Phys. Rev. Lett. **57**, 13 (1986).
[28] A. I. Lvovsky, H. Hansen, T. Aichele, O. Benson, J. Mlynek, and S. Schiller, Quantum State Reconstruction of the Single-Photon Fock State, Phys. Rev. Lett. **87**, 050402 (2001).
[29] A. A. Clerk, M. H. Devoret, S. M. Girvin, F. Marquardt, and R. J. Schoelkopf, Introduction to quantum noise, measurement, and amplification, Rev. Mod. Phys. **82**, 1155 (2010).
[30] D. T. Smithey, M. Beck, M. G. Raymer, and A. Faridani, Measurement of the Wigner Distribution and the Density Matrix of a Light Mode Using Optical Homodyne Tomography: Application to Squeezed States and the Vacuum, Phys. Rev. Lett. **70**, 1244 (1993).
[31] K. Vogel and H. Risken, Determination of quasiprobability distributions in terms of probability distributions for the rotated quadrature phase, Phys. Rev. A **40**, 2847 (1989).
[32] Z. Hradil, Quantum-state estimation, Phys. Rev. A **55**, R1561 (1997).
[33] F. Mallet, M. A. Castellanos-Beltran, H. S. Ku, S. Glancy, E. Knill, K. D. Irwin, G. C. Hilton, L. R. Vale, and K. W. Lehnert, Quantum State Tomography of an Itinerant Squeezed Microwave Field, Phys. Rev. Lett. **106**, 220502 (2011).
[34] M. Christandl and R. Renner, Reliable Quantum State Tomography, Phys. Rev. Lett. **109**, 120403 (2012).
[35] M. S. Kim, F. A. M. De Oliveira, and P. L. Knight, Photon number distributions for squeezed number states and squeezed thermal states, Opt. Commun. **72**, 99 (1989).
[36] D. F. Walls and G. J. Milburn, *Quantum Optics* (Springer Science & Business Media, Berlin, 2007).
[37] J. Řeháček, S. Olivares, D. Mogilevtsev, Z. Hradil, M. G. A. Paris, S. Fornaro, V. D'Auria, A. Porzio, and S. Solimeno, Effective method to estimate multidimensional gaussian states, Phys. Rev. A **79**, 032111 (2009).
[38] A. C. Davison and D. V. Hinkley, *Bootstrap Methods and their Application* (Cambridge University Press, Cambridge, England, 1997), Vol. 1.